Available online at www.sciencedirect.com
SCIENCE DIRECT
Optics Communications 259 (2006) 569–580
OPTICS COMMUNICATIONS
www.elsevier.com/locate/optcom

Linear algorithms for phase retrieval in the Fresnel region. 2. Partially coherent illumination

T.E. Gureyev [a,*], Ya.I. Nesterets [a], D.M. Paganin [a,b], A. Pogany [a], S.W. Wilkins [a]

[a] CSIRO Manufacturing and Infrastructure Technology, Private Bag 33, Clayton South, Vic. 3169, Australia
[b] School of Physics, Monash University, Vic. 3800, Australia

Received 18 June 2005; received in revised form 7 July 2005; accepted 28 September 2005

Abstract

Analytical expressions for the spatial distribution of the spectral density and intensity of projection images are derived for a broad class of object transmission functions in the case of partially coherent Schell-model-type incident illumination. The expressions are linear with respect to the phase distribution in the transmitted wave. Associated methods for phase retrieval are discussed with the emphasis on a technique that allows simultaneous "automatic" phase retrieval and deconvolution of projection images of homogeneous objects by means of mutual cancellation at a specified defocus distance of the Fresnel diffraction effects and the image blurring due to the point-spread function of the imaging system.

PACS: 02.30.Zz; 42.30.Rx; 42.30.Wb; 42.40.−i; 61.10.Dp

Keywords: Inverse problems; Phase retrieval; Image reconstruction; Holography; Theories of diffraction and scattering

1. Introduction

We have recently developed a method [1] for the reconstruction of the phase distribution in the transmitted beam from measured intensity of projection images, that represents a combination of the well-known approaches based on the transport of intensity equation (TIE) and the first Born approximations [2–6]. This phase retrieval method is deterministic and essentially linear with respect to the unknown phase. However, the derivation in [1] was carried out in the context of monochromatic illumination, hence the relevant effects of temporal and spatial coherence properties of the incident illumination have not been investigated. Effects of quasi-homogeneous incident illumination on in-line phase-contrast imaging of objects with slowly varying transfer function have been studied in [7] using the stationary phase method. In the present paper, we extend the method to the case of partially coherent Schell-model-type illumination [8] in order to make it directly applicable for quantitative imaging with realistic sources. Our primary target area of application is X-ray phase-contrast imaging, where the incident illumination is typically produced using either incoherent polychromatic microfocus laboratory sources or synchrotron beamlines utilising bending magnets, undulators or wigglers; all such sources have non-trivial temporal and spatial coherence properties. Recently, several types of new X-ray sources have also been the subject of active research and development (see e.g. [9,10]). In all these cases, the coherence properties of the incident radiation may be affected by various optical elements of the imaging system, such as monochromators, mirrors, lenses, slits, etc. Finally, the effect of the detector system must also be taken into account if quantitative imaging

* Corresponding author. Tel.: +61 3 95452702; fax: +61 3 95441128.
E-mail address: Tim.Gureyev@csiro.au (T.E. Gureyev).

0030-4018/$ - see front matter © 2005 Elsevier B.V. All rights reserved.
doi:10.1016/j.optcom.2005.09.072

or phase retrieval are to be achieved. All these factors are incorporated into the model of the imaging system that is considered in the present paper.

It is well known that in general the expressions for the spectral density and intensity of projection images are non-linear with respect to the phase distribution in the transmitted wave immediately after the object. Typically, this phase distribution needs to be retrieved from the measured intensity data in order to perform quantitative analysis of the sample. This non-linear inverse problem, which is an example of the optical phase retrieval problem, has been investigated under a variety of conditions [6,11,12]. Note that related methods for diffraction tomography have been proposed that do not include an explicit phase retrieval step [13,14], however, equivalent implicit reconstruction of the complex amplitude of the transmitted beam still constitutes an important component in these methods. In the present paper, we demonstrate that in the case where the images are collected in the Fresnel region, the phase retrieval problem can be linearized for a broad class of samples with transmission functions that can be approximated by a sum of a slowly varying function and a rapidly varying function with a small magnitude. Unlike a similar approach originally proposed in [1] here we show that the conditions on the object transmission function should be combined with appropriate conditions on the illuminating wave. An important factor in such an extension is a careful separation of the slowly and rapidly varying components of the phase and intensity of the incident wave, that have to be treated differently [7]. We derive an expression for the spatial distribution of the spectral density and intensity of projection images collected in the Fresnel region as a function of the spectral density distribution of the "effective" source, the slowly varying envelopes of the phase and spectral density of the incident wave in the object plane, the object transmission function and the geometrical parameters of the imaging setup. This expression is linear with respect to the phase of the radiation incident on the object and the phase of the object transmission function. This allows us to present a deterministic non-iterative solution for the phase retrieval problem for images collected in the near-Fresnel region, i.e., the region where the Fresnel number is larger than one. Note that here the Fresnel number is understood as the ratio, $N_F = a^2/(\lambda R')$, of the square of the smallest feature size, a, to the product of the wavelength of the radiation, λ, and the effective defocus distance, R' (see details below).

We also demonstrate that if the phase and logarithm of intensity of the transmitted wave immediately after the object are proportional to each other (this is the case, for example, for uniform illumination of objects consisting of a single material), then a very simple method for "automatic" simultaneous phase retrieval and deconvolution of the projection image originally suggested in the monochromatic case in [15] can be extended to the case of partially coherent Schell-model-type illumination and realistic detector systems. Provided that the images are collected at a specified defocus distance, no post-processing of the images is required in order to achieve both phase retrieval and spatial deconvolution simultaneously. This is because at this defocus distance the blurring of the image due to the total point spread function (PSF) of the imaging system (which incorporates the blurring due to the spectral spread, the finite size of the source, the detector PSF and the geometrical magnification) is cancelled out by the Fresnel diffraction effect. The phenomenon is similar to the Scherzer defocus in electron microscopy [2]. This method quantifies and optimises the well-known fact that in-line phase contrast can sharpen the images even in the case of partially coherent spatial radiation. Consequently, it appears that some effects of the partially coherent illumination that are usually considered detrimental and leading to the loss of image contrast and resolution, can in fact be utilised in a beneficial way to counteract the effects of Fresnel diffraction that can otherwise also degrade the visual quality of projection images. We believe that this approach to optimisation of the performance of projection imaging systems will be useful in a variety of applications using laboratory and synchrotron sources.

2. Projection image contrast under partially coherent illumination

Let a source of an ergodic spatially partially coherent polychromatic beam be located close to the optic axis z upstream from the "source" plane $z = -R_1$ (Fig. 1). We assume that the radiation emitted by the source possibly passes through one or more optical elements before reaching the "object" plane $z = 0$. Let the incident cross-spectral density [8] of the beam in the object plane be equal to $W^{\text{in}}(x,y,x',y',v)\exp[\mathrm{i}k(x'^2 + y'^2 - x^2 - y^2)/(2R_1)]$, where (x,y) and (x',y') are the Cartesian coordinates of two arbitrary points in the object plane, v is the frequency, k is the wavenumber ($k = 2\pi v/c = 2\pi/\lambda$, where c is the speed of light in vacuum) and W^{in} is a function whose properties are determined by the source, the optical elements and the geometrical layout of the illumination system. Here, the exponential factor corresponds to the paraxial approximation of secondary spherical waves "emitted" from individual points in the source plane in accordance with the Huygens–Fresnel principle. As will be seen below, such an explicit inclusion of the parabolic phase term in the description of the incident wavefront is convenient when dealing with small sources.

Let a thin object be located immediately upstream of the object plane $z = 0$ (Fig. 1). The object is characterized by its transmission function $Q(x,y,v)$, $Q = q\exp(\mathrm{i}k\psi)$, where $q \equiv |Q|$. Then the spectral density in the "detector" plane $z = R_2$ can be expressed as a dual Fresnel integral with respect to the spatial arguments, (x,y) and (x',y') [8]

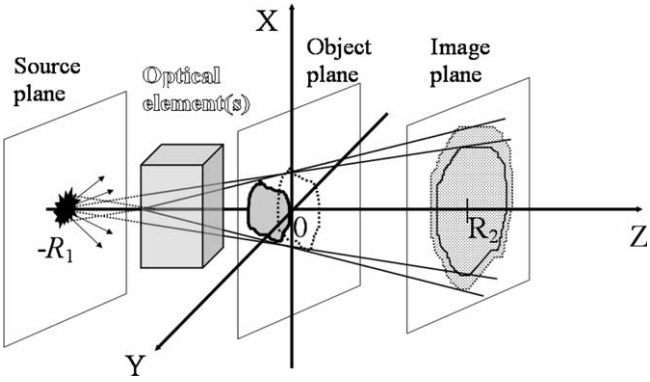

Fig. 1. Schematics of in-line imaging as considered in the present paper, including a polychromatic partially coherent source, possible optical elements making up an illumination system, a thin object and a detector.

$$S(x_2,y_2,R_2,v)=\frac{1}{\lambda^2R_2^2}\int\int\int\int W^{\rm in}(x,y,x',y',v)\,Q^*(x,y,v)\,Q(x',y',v)\times\exp\left\{ik\left[\frac{(x'^2-x^2+y'^2-y^2)}{2R'}+\frac{[x_2(x-x')+y_2(y-y')]}{R_2}\right]\right\}\mathrm{d}x\,\mathrm{d}y\,\mathrm{d}x'\,\mathrm{d}y', \tag{1}$$

where $R'=R_2/M$ is the effective defocus distance and $M=(R_1+R_2)/R_1$ is magnification. It is straightforward to verify that the spatial Fourier transform, $\hat{S}(\xi,\eta,R_2,v)=\int\int\exp[-\mathrm{i}2\pi(x_2\xi+y_2\eta)]S(x_2,y_2,R_2,v)\,\mathrm{d}x_2\,\mathrm{d}y_2$, of the spectral density has the following simple form:

$$\hat{S}\left(\frac{\xi}{M},\frac{\eta}{M},R_2,v\right)=\int\int\exp[-\mathrm{i}2\pi(x\xi+y\eta)]W^{\rm in}(x+\alpha\xi,y+\alpha\eta,x-\alpha\xi,y-\alpha\eta,v)\,Q^*(x+\alpha\xi,y+\alpha\eta,v)\times Q(x-\alpha\xi,y-\alpha\eta,v)\,\mathrm{d}x\,\mathrm{d}y, \tag{2}$$

where $\alpha=\lambda R'/2$. In order to take into account the effect of the detector system, one also needs to multiply Eq. (2) by the modulation transfer function (MTF) of the detector, $\hat{D}(\xi/M,\eta/M,v)$.

Let us consider a model for partially coherent incident illumination which corresponds to a simple generalization of the Schell-model source (for which the spatial coherence properties depend only on the distance between points on the source plane) [8]. We assume that the function $W^{\rm in}$ in the incident cross-spectral density in Eq. (1) has the following form:

$$W^{\rm in}(x,y,x',y',v)=\left[S^{\rm in}(x,y,v)\right]^{1/2}\left[S^{\rm in}(x',y',v)\right]^{1/2}g^{\rm in}(x'-x,y'-y,v)\exp\left\{ik\left[\psi^{\rm in}(x',y',v)-\psi^{\rm in}(x,y,v)\right]\right\}, \tag{3}$$

where $g^{\rm in}(0,0,v)=1$ by definition at all frequencies. Setting $x'=x$ and $y'=y$ in Eq. (3) we see that $W^{\rm in}(x,y,x,y,v)=S^{\rm in}(x,y,v)$, i.e., the function $S^{\rm in}(x,y,v)$ coincides with the incident spectral density distribution in the object plane. Then, by definition [8], the incident spectral degree of coherence in the object plane is equal to $g^{\rm in}(x'-x,y'-y,v)\times\exp\{ik[\psi^{\rm in}(x',y',v)-\psi^{\rm in}(x,y,v)]\}\exp[ik(x'^2+y'^2-x^2-y^2)/(2R_1)]$. Hence, Eq. (3) implies that, similarly to the case of a Schell-model source, the absolute value of the spectral degree of coherence in the object plane, $|g^{\rm in}(x'-x,y'-y,v)|$, depends only on the distance between points in the object plane. When $\psi^{\rm in}\equiv 0$ and $R_1\to\infty$, Eq. (3) exactly corresponds to the cross-spectral density of a Schell-model source [8]. In our model, apart from the explicit parabolic phase factor, we allowed for an additional incident phase term, $k\psi^{\rm in}$, to be present in the incident wave. This term may describe, for example, aberrations of the optical elements of the illumination system. It is instructive to note that the model of incident illumination defined by Eq. (3) includes a number of important practical cases, such as the polychromatic plane and spherical incident waves, radiation from extended spatially incoherent sources, as well as incident illumination from bending magnets at synchrotrons [16]. Natural generalizations of some of these cases, i.e., quasi-plane and quasi-spherical incident waves and radiation from quasi-homogeneous sources also represent special cases of the model defined in Eq. (3) [7]. When $\psi^{\rm in}\equiv 0$ and also the incident spectral density is a slowly varying function of transverse spatial coordinates, so that the approximation $[S^{\rm in}(x,y,v)]^{1/2}[S^{\rm in}(x',y',v)]^{1/2}\cong S^{\rm in}((x'+x)/2,(y'+y)/2,v)$ can be applied, then the expression in Eq. (3) corresponds to the cross-spectral density in the case of a quasi-homogeneous secondary source [8]. We will consider these special cases in more detail in the next section after deriving the desired linearized approximation for the spectral density distribution in the object plane.

It is convenient to introduce a function $S_n^{\rm src}$ which is a rescaled inverse Fourier transform of $g^{\rm in}$

$$g^{\rm in}(x,y,v)=\int\int\exp\left[-\mathrm{i}2\pi\left(\frac{xx'+yy'}{\lambda R_1}\right)\right]S_n^{\rm src}(x',y',v)\mathrm{d}x'\,\mathrm{d}y'. \tag{4}$$

The function S_n^{src} is a normalised version of Hopkins's "effective source" [17], i.e., the theoretical source that creates incident illumination with the degree of coherence equal to g^{in} in the far-field. The normalization simply means that the integral of S_n^{src} over the spatial coordinates (x', y') is equal to one, which immediately follows from Eq. (4) and the fact that $g^{\mathrm{in}}(0,0,v) = 1$. Note that at least for large source-to-object distances R_1 and quasi-homogeneous sources with narrow spatial distribution of the spectral degree of coherence, the function S_n^{src} coincides with the actual normalized spectral density distribution in the source plane in agreement with the van Cittert–Zernike theorem [8].

Substituting Eq. (3) into Eq. (2) and taking into account Eq. (4) and the detector MTF, we obtain

$$\hat{S}(\xi,\eta,R_2,v) = \hat{P}(\xi,\eta,M,v)\hat{S}^{\mathrm{coh}}(M\xi,M\eta,R',v), \tag{5}$$

where $\hat{P}(\xi,\eta,M,v)$ is the total MTF of the system

$$\hat{P}(\xi,\eta,M,v) = \hat{S}_n^{\mathrm{src}}(-(M-1)\xi,-(M-1)\eta,v)\hat{D}(\xi,\eta,v), \tag{6}$$

$$\hat{S}^{\mathrm{coh}}(\xi,\eta,R',v) = \int\int \exp[-\mathrm{i}2\pi(x\xi+y\eta)]\,\tilde{Q}^*(x+\alpha\xi,y+\alpha\eta,v)\,\tilde{Q}(x-\alpha\xi,y-\alpha\eta,v)\,\mathrm{d}x\,\mathrm{d}y, \tag{7}$$

and $\tilde{Q} \equiv (S^{\mathrm{in}})^{1/2}\exp(\mathrm{i}k\psi^{\mathrm{in}})Q$ is the object transmission function modified to take into account the incident spectral density and phase. The MTF of the system, $\hat{P}$, reflects the properties of the source and the detector, as well as the geometrical parameters R_1 and R_2. Comparing Eq. (2) with Eq. (7) one can see that the function $\hat{S}^{\mathrm{coh}}$ corresponds to the Fourier transform of the spectral density in the detector plane in the case of a coherent illumination, $g^{\mathrm{in}}(x,y,v) \equiv 1$. Therefore, Eq. (5) is a direct generalization (written in a Fourier space representation) to the case of a Schell-model-type incident illumination (defined in Eq. (3)) of a well-known formula which states that the image spectral density in the case of a spatially incoherent source is a convolution of the spectral density distribution of the source and the PSF of the detector with the coherent image formed with a point source and an ideal detector. Note that the minus sign appearing in the arguments of the function $\hat{S}_n^{\mathrm{src}}$ in Eq. (6) corresponds to the fact that the spectral density distribution in the detector plane is inverted with respect to the source (in agreement with the usual ray-optics picture of image formation). A result resembling Eqs. (5)–(7) was recently stated in [18]. A similar equation was also obtained earlier in [19].

Taking the inverse Fourier transform of Eq. (5), we can obtain an expression for the spectral density in the detector plane as a function of transverse spatial coordinates (x,y)

$$S(x,y,R_2,v) = M^{-2}\int\int S^{\mathrm{coh}}(x''/M,y''/M,R',v)P(x-x'',y-y'',M,v)\mathrm{d}x''\,\mathrm{d}y'', \tag{8}$$

where

$$P(x,y,M,v) = \int\int S_n^{\mathrm{src}}(x',y',v)D(x+(M-1)x',y+(M-1)y',v)\,\mathrm{d}x'\,\mathrm{d}y' \tag{9}$$

is the total PSF of the system and $S^{\mathrm{coh}}(x,y,R',v)$ is the corresponding spectral density distribution in the case of coherent incident illumination. The last function is equal to the inverse Fourier transform of the function $\hat{S}^{\mathrm{coh}}(\xi,\eta,R',v)$ defined by Eq. (7). Eq. (8) can be interpreted in the conventional way as a convolution of the PSF of the imaging system with the coherent image corresponding to a point source.

Integrating Eq. (8) over v we obtain the following expression for the time-averaged intensity distribution in the detector plane:

$$\begin{aligned} I(x,y,R_2) = M^{-2}\int\int\int\int\int S^{\mathrm{coh}}\left(\frac{x''+(M-1)x'}{M},\frac{y''+(M-1)y'}{M},R',v\right) \\ \times S_n^{\mathrm{src}}(x',y',v)D(x-x'',y-y'',v)\mathrm{d}x'\,\mathrm{d}y'\,\mathrm{d}x''\,\mathrm{d}y''\,\mathrm{d}v. \end{aligned} \tag{10}$$

Having obtained the general formulae, Eqs. (5)–(10) for the spatial distribution of the spectral density and intensity of a projection image under the Schell-model-type illumination satisfying Eq. (3), we now consider relevant properties of the object under investigation. We can always represent any modified transmission function as $\tilde{Q} = \exp(-\tilde{\mu} + \mathrm{i}\tilde{\varphi})$, where $\tilde{\mu}$ and $\tilde{\varphi}$ are real functions. Note that in general Eqs. (5)–(10) are non-linear with respect to the phase $\tilde{\varphi}$. One would have to solve this non-linear equation in order to analyse the distribution of the refractive index in the sample on the basis of measurements of the transmitted spectral density. If one is able to linearize Eqs. (5)–(10) with respect to the phase, the solution to the latter inverse problem is likely to become much simpler. We now proceed with a formulation of conditions on the incident illumination and the object transmission function that will allow us to derive a linear approximation to Eqs. (5)–(10), similar to the one proposed in [1]. This approximation represents a combination of the well-known TIE and first Born approximations [2], but imposes less restrictive conditions on the sample and the incident illumination.

Let d' be the spatial resolution limit of the imaging system in Fig. 1. The value of d' is determined by the spatial and temporal coherence properties of the source, as well as by the geometric parameters R_1 and R_2 and the properties of

the detector system. In particular, it follows from Eq. (5) that if the system's MTF is negligibly small for all (ξ,η) such that $(\xi^2+\eta^2)^{1/2} > 1/d_1$, then $d' \geqslant d_1/M$. Let $1/d''$ be twice the minimal radius of a sphere, with centre at the origin of coordinates in Fourier space, outside which the spatial Fourier transform of $\tilde{Q}$ is negligibly small in magnitude. It can be then shown (e.g., by substituting the spatial Fourier transform of $\tilde{Q}$ into Eq. (7)) that $\hat{S}^{\mathrm{coh}}(\xi,\eta,R',v)$ is negligibly small for all ξ and η such that $(\xi^2+\eta^2)^{1/2} > 1/d''$. We set $d = \min(d',d'')$, choose a length h such that

$$h \geqslant \lambda R'/d \tag{11}$$

and calculate the running averages $\bar{\mu}_h$ and $\bar{\varphi}_h$ of the functions $\tilde{\mu}$ and $\tilde{\varphi}$, according to the following equation:

$$\bar{f}_h(x,y,v) = h^{-2}\int_{-h/2}^{h/2}\int_{-h/2}^{h/2} f(x+x',y+y',v)\,\mathrm{d}x'\,\mathrm{d}y'. \tag{12}$$

The running average $\bar{f}_h$ of an arbitrary function f is always a slowly varying function on length scales smaller than h. The most important assumption that we make about the modified transmission function $\tilde{Q}$ is that the remainders, $\Delta\mu_h \equiv \tilde{\mu} - \bar{\mu}_h$ and $\Delta\varphi_h \equiv \tilde{\varphi} - \bar{\varphi}_h$, are small

$$|\Delta\mu_h(x,y,v)| \ll 1 \quad \text{and} \quad |\Delta\varphi_h(x,y,v)| \ll 1. \tag{13}$$

At the same time, we do not impose any limits on the rate of spatial variation of these remainders. Accordingly, we can now represent the modified transmission function in the following form:

$$\tilde{Q} = Q_h(1+\chi_h), \tag{14}$$

where $Q_h = \exp(-\bar{\mu}_h + \mathrm{i}\bar{\varphi}_h)$ is a slowly varying function and $\chi_h = -\Delta\mu_h + \mathrm{i}\Delta\varphi_h$ is a small one, i.e., $|\chi_h| \ll 1$. Note that the TIE and the first Born approximations correspond to the special cases of Eq. (14) with $\chi_h \equiv 0$ and $Q_h \equiv$ constant, respectively.

Let us substitute Eq. (14) into Eq. (7) and use the properties of the functions Q_h and χ_h to linearize the resultant equation. Firstly, let us use the fact that Q_h is a slowly varying function to replace the functions Q_h^* and Q_h by their first-order Taylor approximations

$$Q_h^*(x+\lambda R'\xi/2, y+\lambda R'\eta/2, v) \cong Q_h^*(x,y,v) + \lambda R'\left[\xi\partial_x Q_h^*(x,y,v) + \eta\partial_y Q_h^*(x,y,v)\right]/2 \tag{15}$$

and similarly for Q_h. These approximations are valid for any (ξ,η) such that $(\xi^2+\eta^2) \leqslant d^{-2}$, because then $\lambda R'(\xi^2+\eta^2)^{1/2} \leqslant \lambda R'/d \leqslant h$ according to Eq. (11), and hence the function Q_h is indeed slowly varying over the relevant ranges of its spatial arguments. After substituting Eq. (15) into Eq. (7), we use the identities $\xi\exp[-\mathrm{i}2\pi(x\xi+y\eta)] = (\mathrm{i}/2\pi)\partial_x\exp[-\mathrm{i}2\pi(x\xi+y\eta)]$ and $\eta\exp[-\mathrm{i}2\pi(x\xi+y\eta)] = (\mathrm{i}/2\pi)\partial_y\exp[-\mathrm{i}2\pi(x\xi+y\eta)]$, and then integrate by parts to obtain

$$\begin{aligned}\hat{S}^{\mathrm{coh}}(\xi,\eta,R',v) = \int\int \exp[-\mathrm{i}2\pi(x\xi+y\eta)]\Big\{&\left[|Q_h|^2 - (\mathrm{i}R'/k)\nabla_\perp\cdot\mathrm{Im}(Q_h\nabla_\perp Q_h^*)\right](x,y,v)\\ &+\left(|Q_h|^2\chi_h^*\right)(x+\alpha\xi,y+\alpha\eta,v) + (|Q_h|^2\chi_h)(x-\alpha\xi,y-\alpha\eta,v)\Big\}\mathrm{d}x\,\mathrm{d}y.\end{aligned} \tag{16}$$

In the derivation of Eq. (16), we have also made use of the fact that both χ_h and the second term on the right-hand side of Eq. (15) are much smaller than unity, which allowed us to discard the expressions containing products of these terms. Now we substitute the expressions $Q_h = q_h\exp(\mathrm{i}\bar{\varphi}_h)(q_h \equiv \exp(-\bar{\mu}_h))$ and $\chi_h = -\Delta\mu_h + \mathrm{i}\Delta\varphi_h$ into Eq. (16) to obtain

$$\begin{aligned}\hat{S}^{\mathrm{coh}}(\xi,\eta,R',v) = \Big\{&[q_h^2]^\wedge(\xi,\eta,v) - (R'/k)[\nabla_\perp\cdot(q_h^2\nabla_\perp\bar{\varphi}_h)]^\wedge(\xi,\eta,v)\\ &-2\cos[\pi\lambda R'(\xi^2+\eta^2)]\left[q_h^2\Delta\mu_h\right]^\wedge(\xi,\eta,v) + 2\sin[\pi\lambda R'(\xi^2+\eta^2)][q_h^2\Delta\varphi_h]^\wedge(\xi,\eta,v)\Big\},\end{aligned} \tag{17}$$

where the hat symbol, "$\wedge$", denotes the spatial Fourier transform (as defined above after Eq. (1)) of the preceding expression in square brackets. The first line of Eq. (17) corresponds to the TIE-type approximation applied to the slowly varying function $Q_h = q_h\exp(\mathrm{i}\bar{\varphi}_h)$, while the second line corresponds to the scattered wave in the first Born type approximation applied to the function $|Q_h|^2\chi_h = -q_h^2\Delta\mu_h + \mathrm{i}q_h^2\Delta\varphi_h$.

Taking the inverse Fourier transform of Eq. (17), we can obtain an expression for the spectral density in the detector plane in the case of coherent illumination

$$\begin{aligned}S^{\mathrm{coh}}(x,y,R',v) = {}& q_h^2(x,y,v) - (R'/k)\left[\nabla_\perp\cdot(q_h^2\nabla_\perp\bar{\varphi}_h)\right](x,y,v)\\ &-[2/(\lambda R')]\int\int\Big\{\sin\left[\pi(x'^2+y'^2)/(\lambda R')\right][q_h^2\Delta\mu_h](x-x',y-y',v)\\ &-\cos[\pi(x'^2+y'^2)/(\lambda R')][q_h^2\Delta\varphi_h](x-x',y-y',v)\Big\}\mathrm{d}x'\,\mathrm{d}y'.\end{aligned} \tag{18}$$

Eq. (18) is obviously linear with respect to the phase $\tilde{\varphi} \equiv \bar{\varphi}_h + \Delta\varphi_h$. Note that both the phase and the intensity terms present in Eq. (18) contain contributions from the incident wave, as well as the object, as by definition $\tilde{\varphi} = k\psi^{\text{in}} + \arg Q$ and $\tilde{\mu} = -\ln(S^{\text{in}})/2 - \ln|Q|$.

3. Special cases

In this section, we consider several important special cases of Eqs. (5)–(10), (17) and (18) which occur in practice when a particular type of imaging system is employed or a particular class of samples is investigated.

We first consider the illumination conditions. Eqs. (5)–(10), (17) and (18) have been obtained using a rather general model of partially coherent incident illumination described by Eq. (3). Later in Eq. (13), we imposed additional restrictions on the incident distributions of spectral density and phase. Eq. (13) requires that these distributions, $\ln S^{\text{in}}$ and $k\psi^{\text{in}}$, can be approximated by slowly varying functions, $\ln S_h^{\text{in}}$ and $k\psi_h^{\text{in}}$, with the remainders, $|\ln S^{\text{in}} - \ln S_h^{\text{in}}|$ and $|k(\psi^{\text{in}} - \psi_h^{\text{in}}|)$, both being much smaller than unity. The shortest scale of variation, h, of the slowly varying components $\ln S_h^{\text{in}}$ and $k\psi_h^{\text{in}}$ must satisfy Eq. (11). We previously noted that the model of incident illumination described by Eq. (3) includes the cases of plane and spherical incident waves, as well as radiation from extended spatially incoherent sources. Let us now see how Eqs. (17) and (18) look in these particular cases.

(1) As noted earlier, when $\psi^{\text{in}} \equiv 0$, Eq. (3) corresponds to the case of a Schell-model illumination. When additionally S^{in} is a slowly varying function such that $[S^{\text{in}}(x,y,v)]^{1/2}[S^{\text{in}}(x',y',v)]^{1/2} \cong S^{\text{in}}((x'+x)/2,(y'+y)/2,v)$, Eq. (3) corresponds to a quasi-homogeneous source, with Eqs. (5)–(10), (17) and (18) describing the corresponding spectral density and time-averaged polychromatic intensity distributions in the image plane. Finally, when $S^{\text{in}}(x,y,v) = S^{\text{in}}(v)$, Eq. (8) together with Eq. (18) becomes a combined TIE + Born equation [1] for an extended spatially incoherent source where the image is a convolution of the spectral density distribution in the source plane and the detector PSF with a coherent image formed with a point source. Note that the linearization is not essential to the forgoing; a similar result will apply to the general $\hat{S}^{\text{coh}}$ of Eq. (5).

(2) When $S_n^{\text{src}}(x,y,v) = \delta(x - x_1)\delta(y - y_1)$, Eq. (8) trivially reduces to a convolution of the detector PSF with Eq. (18) divided by M^2 and evaluated at the point $([x'' + (M-1)x_1]/M, [y'' + (M-1)y_1]/M, R', v)$. This corresponds to the case of a quasi-spherical incident wave from a small spatially coherent source with centre located at the point $(x_1, y_1, -R_1)$. In particular, when one also has $\psi^{\text{in}} \equiv 0$ and $S^{\text{in}}(x,y,v) = S^{\text{in}}(v)$, Eq. (8) with Eq. (18) transforms into the combined TIE + Born equation for a point source.

(3) When $M = 1$, Eq. (8) reduces to a convolution of the detector PSF with Eq. (18), with R' replaced by R_2, i.e., it transforms into an equation describing the spectral density distribution of an in-line image in the case of a quasi-plane incident wave. In particular, when one also has $\psi^{\text{in}} \equiv 0$ and $S^{\text{in}}(x,y,v) = S^{\text{in}}(v)$, Eq. (17) transforms into the conventional TIE+Born equation for a plane wave obtained earlier in [1] in the case of a coherent plane incident wave.

Now we shift our attention to special classes of samples. We have previously assumed that a sample under investigation is fully characterised by its transfer function, $Q(x,y,v) = q(x,y,v)\exp[ik\psi(x,y,v)]$. Here, we consider two important special classes of such samples, namely those with negligible absorption (“pure phase” samples) and those consisting predominantly of a single material (“homogeneous” samples) [20]. For pure phase samples one has $q(x,y,v) \equiv 1$, while homogeneous samples are characterized by the proportionality relationship between the attenuation and phase, $k\psi(x,y,v) = \gamma(v)\ln q(x,y,v)$ (the proportionality constant $\gamma(v)$ is equal to the ratio of the real to the imaginary part of the complex refractive index $n(v)$ of the object, i.e., $\gamma \equiv \delta/\beta, n = 1 - \delta + i\beta$). In both cases instead of a complex unknown distribution, Q, one has a single real unknown distribution, ψ (the constant $\gamma(v)$ is assumed to be known). Consequently, the equations for projection image contrast can be simplified in these cases. In particular, Eq. (17) in the Fourier space representation takes the following simple form in the case of uniform illumination ($S^{\text{in}}(x,y,v) \equiv S^{\text{in}}(v)$) and pure phase objects

$$\hat{S}^{\text{coh}}(\xi,\eta,R',v) = S^{\text{in}}(v)\Big\{\delta(\xi,\eta) - (R'/k)\big[\nabla_\perp^2 \bar{\varphi}_h\big]^\wedge(\xi,\eta,v) + 2\sin\big[\pi\lambda R'(\xi^2+\eta^2)\big][\Delta\varphi_h]^\wedge(\xi,\eta,v)\Big\}. \tag{19}$$

Taking into account the slowly varying nature of the function $\bar{\varphi}_h$ and the fact that the Fourier transform of $-(R'/k)\nabla_\perp^2$ is equal to $2\pi\lambda R'(\xi^2+\eta^2)$, i.e., to the leading term of the Taylor expansion of the sine function in the last term of Eq. (19), it is possible to merge the second and third terms of Eq. (19) into a single expression

$$\hat{S}^{\text{coh}}(\xi,\eta,R',v) = S^{\text{in}}(v)\Big\{\delta(\xi,\eta) + 2\sin\big[\pi\lambda R'(\xi^2+\eta^2)\big]\hat{\tilde{\varphi}}(\xi,\eta,v)\Big\}. \tag{20}$$

Note that Eq. (20) is expressed in terms of the total phase function, $\tilde{\varphi} \equiv \bar{\varphi}_h + \Delta\varphi_h = k(\psi^{\text{in}} + \psi)$. This result was first obtained by Guigay [21], with the validity conditions expressed in the form $|\varphi(x+\alpha\xi, y+\alpha\eta, v) - \varphi(x-\alpha\xi, y-\alpha\eta, v)| \ll 1$, where $\alpha = \lambda R'/2$ as above (see also [22]).

In the case of a uniform illumination ($S^{\mathrm{in}}(x,y,v) \equiv S^{\mathrm{in}}(v)$) with $\psi^{\mathrm{in}}(x,y,v) \equiv 0$ and a homogeneous object we obtain from Eq. (17)

$$\hat{S}^{\mathrm{coh}}(\xi,\eta,R',v) = [q_h^2]^{\wedge}(\xi,\eta,v)\{1+\gamma\pi\lambda R'(\xi^2+\eta^2)\} - 2[q_h^2\Delta\mu]^{\wedge}(\xi,\eta,v)\{\cos[\pi\lambda R'(\xi^2+\eta^2)] + \gamma\sin[\pi\lambda R'(\xi^2+\eta^2)]\}. \tag{21}$$

This result was first obtained in [1], here we have presented it in a slightly different (equivalent) form. Noting that $\cos\theta + \gamma\sin\theta \to 1+\gamma\theta$ when θ tends to zero, and proceeding similarly to the derivation of Eq. (20) we can simplify Eq. (21)

$$\hat{S}^{\mathrm{coh}}(\xi,\eta,R',v) = \mathrm{S}^{\mathrm{in}}(v)[q^2]^{\wedge}(\xi,\eta,v)\{\cos[\pi\lambda R'(\xi^2+\eta^2)] + \gamma\sin[\pi\lambda R'(\xi^2+\eta^2)]\}. \tag{22}$$

Eq. (22) is expressed in terms of the total modulus of the transmission function $q = \exp(-\bar{\mu}_h - \Delta\mu_h)$. This result represents an extension of the results obtained earlier for slowly varying homogeneous objects in [20], for weak objects in [23] and for objects with weak absorption and with the phase shifts satisfying the Guigay condition (see above after Eq. (20)) in [22].

Eq. (22) transforms into Eq. (20) when $\gamma \to \infty$, i.e., for pure phase objects. In order to verify the latter limit it is sufficient to use the identity $[q^2]^{\wedge}(\xi,\eta,v) \cong \delta(\xi,\eta) + 2\gamma^{-1}\hat{\varphi}(\xi,\eta,v)$ which is valid when $\gamma \to \infty$. Even more importantly, at large but finite values of γ Eq. (22) represents a natural Tikhonov-type regularization of Eq. (20), and as a consequence Eq. (22) is very stable with respect to noise in the experimental images at low spatial frequencies [24]. Indeed, Eq. (22) implies

$$[\exp(2\gamma^{-1}\varphi)]^{\wedge}(\xi,\eta,v) \cong \frac{\hat{S}^{\mathrm{coh}}(\xi,\eta,R',v)}{S^{\mathrm{in}}(v)\{\cos[\pi\lambda R'(\xi^2+\eta^2)] + \gamma\sin[\pi\lambda R'(\xi^2+\eta^2)]\}}. \tag{23}$$

The denominator in Eq. (23) is sufficiently different from zero at low spatial frequencies. Therefore, the presence of absorption in the object increases the robustness of phase retrieval from projection images. This point is developed further in the next section, where we consider the effects of partially coherent illumination and detector PSF on phase retrieval in the case of homogeneous samples.

We should mention, however, that the numerical experiments that we have performed so far seem to indicate that at least for slowly varying transmission functions, Eq. (23) tends to produce less accurate results than the original equation from [20] (i.e., the equation that can be obtained from Eq. (23) by replacing *cos* by 1 and *sin* by its argument in the denominator). Note that in the latter case Eq. (23) and its simplified version from [20] both represent valid, but *different*, approximations to the full non-linear equation for the object-plane phase distribution. The accuracy of the two approximations may need to be compared and analysed in more detail in the future.

4. Phase retrieval in the near-Fresnel region with partially coherent illumination

In an earlier paper [1], we have discussed linear methods for phase retrieval in the near-Fresnel region. These methods were based on a model similar to Eq. (14) in the case of a plane monochromatic incident wave. Effectively, in that case we had to solve an equation similar to Eq. (17), but with $\psi^{\mathrm{in}} \equiv 0$ and $S^{\mathrm{in}}(x,y,v) = S^{\mathrm{in}}(v)$, in order to reconstruct the transmission function of the object. In the case of partially coherent illumination that is considered in the present paper, we can reduce the problem to the one solved earlier in the coherent case.

Let us first consider Eq. (10). This equation corresponds to experiments in which only the polychromatic time-averaged intensity can be measured for one or several different distributions of the incident spectral density and possibly with different values of geometrical parameters R_1 and R_2. A more favourable situation, where experimental measurements can be performed at individual wavelengths using either quasi-monochromatic incident radiation or energy-resolving detectors, has been studied in detail in [25]. If measurements at individual wavelengths are not available, then often a simplifying assumption is used that the spatial distribution of the source spectral density is approximately the same at all wavelengths, i.e., $S_n^{\mathrm{src}}(x,y,v) = I_n^{\mathrm{src}}(x,y)$. Then the latter spatial distribution can be eliminated from Eq. (10) by means of numerical deconvolution. The effect of the detector PSF can be taken into account in a similar manner. These operations generally require the functions S_n^{src} and D to be known quite accurately, with this knowledge coming either from separate experimental measurements or from computer modelling as was done in [26]. After that one has to deal either with Eq. (17) in the case of monochromatic data or with its integral over v in the polychromatic case. The latter case is, of course, more difficult; a solution to this phase retrieval problem in the TIE approximation for weakly absorbing objects was recently reported in [27]. In the monochromatic case, one only has to solve Eq. (17), i.e., reconstruct the modified object transmission function from the spectral density distribution at a fixed wavelength in the detector plane. Solutions to this problem in the case of a plane incident wave were obtained in [1] for pure phase objects, objects consisting of a single material or general objects. It was shown that in the first two cases a unique solution can be obtained from a single measurement of the spatial distribution of spectral density at fixed wavelength and distances R_1 and R_2. In the case of a general object with uncorrelated absorption and refraction properties, a single measurement of this kind is insufficient, and at least two measurements

are required either at different values of the defocus distance R' or at two different radiation wavelengths. The main difference between the problems considered in [1] and similar ones naturally arising in the present context is in the existence of non-trivial distributions of the incident phase and spectral density distributions, $\psi^{\rm in}$ and $S^{\rm in}$, which are "mixed up" with the object transmission function. Generally, this requires an additional experiment for quantitative characterization of the incident illumination to be performed prior to the experiments with "unknown" samples. The characterization experiment would consist of measurements of the "flat field" images (images without any samples) at the same wavelengths that will later be used for analysis of samples. The spectral density distribution over the detector plane has to be measured at two or three different defocus distances R' [6]. These experimental data can then be used to reconstruct the functions $\psi^{\rm in} = \overline{\psi}^{\rm in}_h + \Delta\psi^{\rm in}$ and $\ln S^{\rm in} = \ln S^{\rm in}_h + \Delta \ln S^{\rm in}$, e.g., using the method proposed in [1] for general objects. After that, one is able to perform experiments with unknown samples, recover the modified transmission function, $\tilde{Q} \equiv (S^{\rm in})^{1/2}\exp(ik\psi^{\rm in})Q$, and use the identities $\arg Q = \arg\tilde{Q} - k\psi^{\rm in}$ and $|Q| = |\tilde{Q}|/(S^{\rm in})^{1/2}$ for the reconstruction of the unknown object transmission function.

In view of the above arguments it appears unnecessary to reproduce here the phase retrieval formulas already described in detail in [1], and elsewhere, in the case of coherent illumination. In order to make use of these results in the case of partially coherent illumination satisfying the model of Eq. (3), one need only combine the steps described in the previous paragraph with the results from [1]. Perhaps, a less well-known method for phase retrieval relevant to the main topic of the present paper was recently proposed in [15]. There a novel method for simultaneous "hardware" phase retrieval and deconvolution was developed in the context of monochromatic illumination. Here, we extend this method to partially coherent illumination described by Eq. (3).

Consider the following expression for the spectral density distribution in the detector plane that can be obtained in the case of uniform incident illumination of a homogeneous object from Eqs. (5) and (22)

$$\hat{S}(\xi,\eta,R_2,\nu) = S^{\rm in}(\nu)[q^2]^\wedge(M\xi,M\eta,R',\nu)\hat{P}(\xi,\eta,M,\nu)\left\{\cos\left[\pi\lambda R'M^2(\xi^2+\eta^2)\right] + \gamma\sin\left[\pi\lambda R'M^2(\xi^2+\eta^2)\right]\right\}. \tag{24}$$

The corresponding "coherent" contrast transfer function (CTF) for homogeneous objects, $C^{\rm coh}(M\xi,M\eta,R',\nu) \equiv \cos[\pi\lambda R'M^2(\xi^2+\eta^2)] + \gamma\sin[\pi\lambda R'M^2(\xi^2+\eta^2)]$, is shown in Fig. 2 for $M = 1$, $\lambda = 0.1$ nm, $\gamma = 68.7$ and $R' = 2.84$ cm (except for M, the same parameter values are used in numerical simulations below). Also shown in Fig. 2 are the corresponding "partially coherent" CTF $C(\xi,\eta,R',\nu) = \hat{P}(\xi,\eta,M,\nu)C^{\rm coh}(M\xi,M\eta,R',\nu)$ and the system's MTF, $\hat{P}(\xi,\eta,M,\nu)$. There we assumed that the MTF has the form $\hat{P}(\xi,\eta,M,\nu) \cong [1+\gamma\pi\lambda R'M^2(\xi^2+\eta^2)]^{-1}$. As one can see, in this case the combined "partially coherent" CTF is flat at low spatial frequencies. This indicates that the corresponding imaging system is free from low-order aberrations. Let us consider this point in more detail for a broader class of system MTFs.

As explained above, the expression $\cos[\pi\lambda R'M^2(\xi^2+\eta^2)] + \gamma\sin[\pi\lambda R'M^2(\xi^2+\eta^2)]$ in Eq. (24) can be replaced by $1 + \gamma\pi\lambda R'M^2(\xi^2+\eta^2)$ in the case of slowly varying transmission functions. We also assume that the system's MTF is a slowly varying function on the "length" scale M/d. In other words, we make an assumption that the spatial resolution of the system is well matched with the finest structure details in the object. Then the MTF can be approximated by the second-order Taylor expansion, $\hat{P}(\xi,\eta,M,\nu) \cong \sum_{m=0}^{2}\sum_{n=0}^{2-m}\frac{1}{m!n!}\partial_\xi^m\partial_\eta^n\hat{P}(0,0,M,\nu)\xi^m\eta^n$. It is easy to see, that the partial derivatives of the MTF in the Taylor expansion coincide with the moments of the PSF [15,28], i.e., $\partial_\xi^m\partial_\eta^n\hat{P}(0,0,M,\nu) = (2\pi i)^{m+n}m!n!p_{mn}(M,\nu)$, where

$$p_{mn}(M,\nu) \equiv \frac{(-1)^{m+n}}{m!n!}\int\int x^m y^n P(x,y,M,\nu)\,{\rm d}x\,{\rm d}y. \tag{25}$$

We assume that the PSF is symmetric, so that $p_{01} = p_{10} = p_{11} = 0$ and $p_{02} = p_{20} > 0$. We denote the latter second-order moment by $p_2 \equiv p_{20}$ and denote $p_0 \equiv p_{00}$. Then $\hat{P}(\xi,\eta,M,\nu) \cong p_0(M,\nu) - (2\pi)^2 p_2(M,\nu)(\xi^2+\eta^2)$, where the second term on the

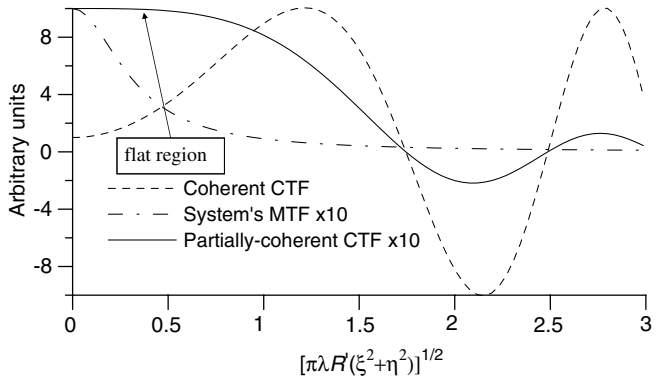

Fig. 2. Coherent and partially coherent contrast transfer functions for homogeneous objects, together with the system's MTF.

right-hand side is much smaller than the first one as long as $\xi^2+\eta^2 \leqslant M^2 d^{-2}$ according to the assumption made above about the slowly varying nature of the system's MTF. Using this fact and Eq. (11) we derive from Eq. (24):

$$\hat{S}(\xi,\eta,R_2,\nu) = [q_h^2]^{\wedge}(M\xi,M\eta,\nu)\Big\{p_0(M,\nu) + (\xi^2+\eta^2)\Big[\gamma\pi\lambda R' M^2 p_0(M,\nu) - (2\pi)^2 p_2(M,\nu)\Big]\Big\}. \tag{26}$$

A simple formula for phase retrieval which represents an extension of the main result from [20] to the case of partially coherent illumination follows directly from Eq. (26):

$$[\exp(2\gamma^{-1}\varphi_h)]^{\wedge}(\xi,\eta,\nu) = \frac{\hat{S}(\xi/M,\eta/M,R_2,\nu)}{p_0(M,\nu) + (\xi^2+\eta^2)[\gamma\pi\lambda R' p_0(M,\nu) - (2\pi)^2 M^{-2} p_2(M,\nu)]}. \tag{27}$$

In order for the phase retrieval formula to be stable with respect to noise in the measured spectral density distribution in the detector plane, the denominator in Eq. (27) should be sufficiently different from zero for all ξ and η. Normally $p_0(M,\nu) > 0$, so the robustness condition becomes $\gamma R' p_0(M,\nu) \geqslant 2kM^{-2}p_2(M,\nu)$. Note that in the case of coherent illumination and ideal detector we have $p_2(M,\nu) = 0$, and so the robustness condition is fulfilled [20]. In the general partially coherent case the phase retrieval algorithm, Eq. (27), is stable with respect to noise in the input data as long as the PSF of the imaging system is sufficiently narrow to ensure that phase-contrast information is available in the measured image data (i.e., the Fresnel fringes are not completely washed out by convolution with the PSF). Finally, when $\gamma R' p_0(M,\nu) = 2kM^{-2}p_2(M,\nu)$, the term in square brackets in Eq. (26) vanishes. Let

$$R'_{\mathrm{d}}(M,\nu) \equiv M^{-2}k\sigma^2(M,\nu)/\gamma(\nu), \tag{28}$$

where $\sigma \equiv (2p_2/p_0)^{1/2}$ is the standard deviation of the PSF. Note also that $\sigma^2(M,\nu) = \sigma_{\mathrm{D}}^2(M,\nu) + (M-1)^2\sigma_{\mathrm{S}}^2(M,\nu)$, where σ_{D} and σ_{S} correspond to the PSF of the detector and the source, respectively. At the defocus distance R'_{d} the spectral density distribution becomes simply

$$\hat{S}(\xi,\eta,MR'_{\mathrm{d}},\nu) \cong [q_h^2]^{\wedge}(M\xi,M\eta,\nu)p_0(M,\nu), \tag{29}$$

i.e., the image coincides with the rescaled modified transmission function. The effects of the convolution with the system PSF and the Fresnel diffraction have cancelled each other. This condition is analogous to the Scherzer defocus in electron microscopy [2], where Fresnel diffraction effects are optimally cancelled by the spherical aberration of an electron microscope. The phase retrieval algorithm becomes trivial in this case, as can be easily seen from Eqs. (27) and (28).

The cancellation condition in Eq. (28) generally depends on the wavelength, i.e., the optimal defocus distance may be different at different wavelengths. In the case of polychromatic incident radiation a similar condition can be derived [24] at least in the case of uniform illumination ($\psi^{\mathrm{in}} \equiv 0$ and $S^{\mathrm{in}}(x,y,\nu) = S^{\mathrm{in}}(\nu)$) and weakly absorbing objects. The weakness of absorption means that the approximation $|Q(x,y,\nu)|^2 = 1 - 2\mu(x,y,\nu) = 1 - 2k\beta(\nu)T(x,y)$ can be applied for the transmission function, where $T(x,y)$ is the projected thickness of the object. Substituting this into Eq. (26), integrating over ν and taking the inverse Fourier transform with respect to the spatial coordinates, we obtain the following equation for the intensity distribution in projection images:

$$\begin{aligned} M^2 I(Mx,My,R_2) = {} & \int S^{\mathrm{in}}(\nu)p_0(M,\nu)\,\mathrm{d}\nu - T(x,y)\int 2k\beta(\nu)S^{\mathrm{in}}(\nu)p_0(M,\nu)\,\mathrm{d}\nu + \nabla_\perp^2 T(x,y) \\ & \times \int S^{\mathrm{in}}(\nu)\big[\delta(\nu)R' p_0(M,\nu) - 2kM^{-2}\beta(\nu)p_2(M,\nu)\big]\,\mathrm{d}\nu. \end{aligned} \tag{30}$$

The last equation has a simple structure: $M^2 I(Mx,My,R_2) = c_0 - c_1 T(x,y) + c_2\nabla_\perp^2 T(x,y)$, and hence allows the following solution, $\hat{T}(\xi,\eta) = [c_0 - I(\xi/M,\eta/M,R_2)]/[c_1 + c_2(2\pi)^2(\xi^2+\eta^2)]$. The robustness condition here is $c_2 \geqslant 0$, i.e., $\int S^{\mathrm{in}}(\nu)$ $[\delta(\nu)R' p_0(M,\nu) - 2kM^{-2}\beta(\nu)p_2(M,\nu)]\,\mathrm{d}\nu \geqslant 0$, which is an obvious generalization of the robustness condition given above for the monochromatic case. Finally, the intensity distribution of an image measured at the defocus distance

$$R'_{\mathrm{d}} = \frac{2\int k\beta(\nu)p_2(M,\nu)S^{\mathrm{in}}(\nu)\,\mathrm{d}\nu}{M^2\int \delta(\nu)p_0(M,\nu)S^{\mathrm{in}}(\nu)\,\mathrm{d}\nu} \tag{31}$$

is equal to

$$I(Mx,My,MR'_{\mathrm{d}}) \cong M^{-2}\int |Q(x,y,\nu)|^2 p_0(M,\nu)S^{\mathrm{in}}(\nu)\,\mathrm{d}\nu. \tag{32}$$

If the width of the source and the detector PSFs is the same at all wavelengths present in the incident spectrum, then Eq. (31) can be simplified

$$R'_{\mathrm{d}} = \frac{[\sigma_{\mathrm{D}}^2 + (M-1)^2\sigma_{\mathrm{S}}^2]}{M^2}\,\frac{\langle k\beta\rangle}{\langle\delta\rangle}, \tag{33}$$

where $\langle k\beta\rangle = \int k\beta(\nu)S^{\mathrm{in}}(\nu)\,\mathrm{d}\nu/I^{\mathrm{in}}$, $\langle\delta\rangle = \int\delta(\nu)S^{\mathrm{in}}(\nu)\,\mathrm{d}\nu/I^{\mathrm{in}}$ and $I^{\mathrm{in}} = \int S^{\mathrm{in}}(\nu)\,\mathrm{d}\nu$.

Using equation $\varphi(x,y,v) = -k\delta(v)T(x,y)$ for the transmitted phase in the object plane, it is also possible to derive from Eqs. (30) and (31) the following formula for phase retrieval (at any chosen frequency v_0):

$$\varphi(x,y,v_0) = k_0\delta(v_0)\frac{[M^2 I(Mx,My,MR'_{\rm d}) - \int p_0(M,v)S^{\rm in}(v)\,{\rm d}v]}{2\int k\beta(v)p_0(M,v)S^{\rm in}(v)\,{\rm d}v}. \tag{34}$$

By choosing the defocus distance according to Eq. (28) in the monochromatic case or Eq. (31) or Eq. (33) in the polychromatic case one can achieve "automatic" simultaneous spatial deconvolution and phase retrieval. This result is achieved by making the Fresnel diffraction counteract the blurring due to the finite size of the PSF of the imaging system. Compared to conventional "post-processing" methods for image deconvolution and phase retrieval, the above "hardware" method has an obvious advantage of being insensitive to the image detection noise. The method is also applicable to the problem of "proximity gap" correction in lithography [24].

In order to illustrate this technique we have performed the following numerical simulation. We have considered an incident polychromatic wave with the wavelength spectrum of a tungsten X-ray tube operated at $E = 30$ kV. The corresponding spectral density (Fig. 3) was generated with the help of the XOP Xtubex program [29,30] (note that we have converted the photon flux units into the corresponding power densities). The MTFs of the source and the detector were both modelled as Lorentzians, with the corresponding PSFs having the standard deviations of $\sigma_{\rm S} = 2$ μm and $\sigma_{\rm D} = 10$ μm, respectively. For simplicity we assumed that these PSFs were the same at all wavelengths present in the incident spectrum. The object was assumed to consist of Apatite with a transverse size of 1.6×1.6 mm^2 and with maximum thickness variation of ~50 μm. The latter corresponds to the maximum phase shift of 10 radians and maximum absorption of ~30% (therefore, the object could not be treated within the first Born approximation). The spatial distribution of the object thickness was taken to be proportional to the standard "Lena" image. The distribution of the polychromatic (time-averaged) transmitted intensity in the object plane was calculated using the projection approximation and the known complex refractive index values for Apatite at energies corresponding to the incident spectral density within the range of 6–30 keV with 0.5 keV steps [31]. Fig. 4(a) depicts the spatial distribution of the transmitted time-averaged intensity in the object plane before the convolution with the system's PSF, while Fig. 4(b) shows the same distribution after the convolution with the PSF. The blurring of the image due to the convolution with the PSF is apparent. Note that in the object plane one has $M = 1$ and, hence, $\sigma \equiv \sigma_{\rm D}$, i.e., the blurring due to the source does not affect the image. Assuming the magnification value of $M = 2$, we then calculated the optimal defocus distance $R'_{\rm d}$ according to Eq. (33); it was found to be equal to 2.84 cm. This corresponds to the source-to-object and object-to-detector distances both equal to 5.68 cm. The corresponding projection image was calculated using Kirchhoff integrals for each monochromatic component, before summing up the obtained monochromatic images with weights proportional to the spectral density of the incident radiation at appropriate wavelengths. The standard deviation of the total PSF at $M = 2$ was equal to $\sigma = [\sigma_{\rm D}^2 + (M-1)^2\sigma_{\rm S}^2]^{1/2} = 10.2$ μm. The resultant polychromatic projection image at $R' = 2.84$ cm convolved with the system PSF is shown in Fig. 4(c). It is easy to see that it looks virtually identical to the transmitted intensity distribution in the object plane without the convolution with the PSF, Fig. 4(a). In other words, in agreement with Eqs. (30)–(32), the effect of Fresnel diffraction at this distance

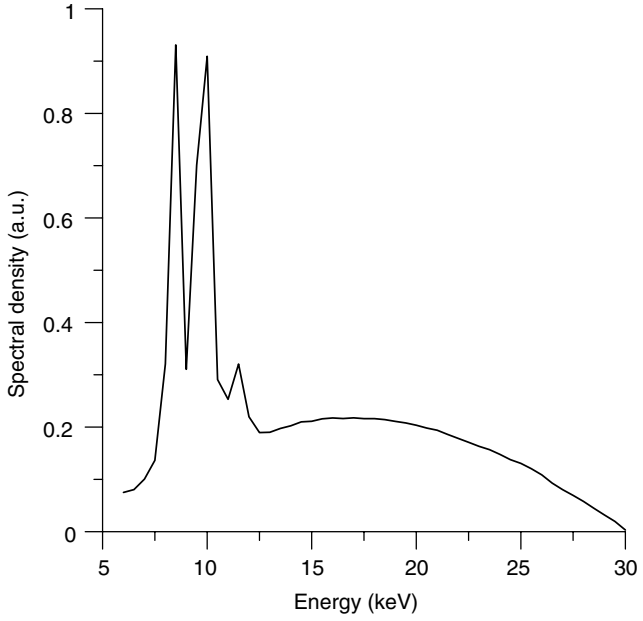

Fig. 3. Spectral density distribution of X-ray radiation from a W tube operated at 30 kV.

Fig. 4. Time-averaged transmitted intensity distribution calculated assuming an extended isotropic X-ray source of approximately 4 μm size and the energy spectrum shown in Fig. 3, the detector PSF of approximately 20 μm size, a homogeneous object consisting of Apatite with a transverse size of $1.6 \times 1.6\ \mathrm{mm}^2$ and with maximum thickness variation of ~50 μm, and different effective defocus distances: (a) $R' = 0$, before the convolution with the system's PSF, (b) $R' = 0$, after the convolution with the system's PSF, (c) $R' = R'_{\mathrm{d}} = 2.84$ cm, after the convolution with the system's PSF, (d) $R' = 28.4$ cm, after the convolution with the system's PSF.

has precisely cancelled the effect of the convolution with the PSF. As an additional illustration we calculated an image at a longer propagation distance of $R' = 28.4$ cm and $M = 2$ (Fig. 4(d)). In this image the Fresnel diffraction already "overwhelms" the effects of convolution with the PSF, and the Fresnel fringes near sharp edges can be observed despite the

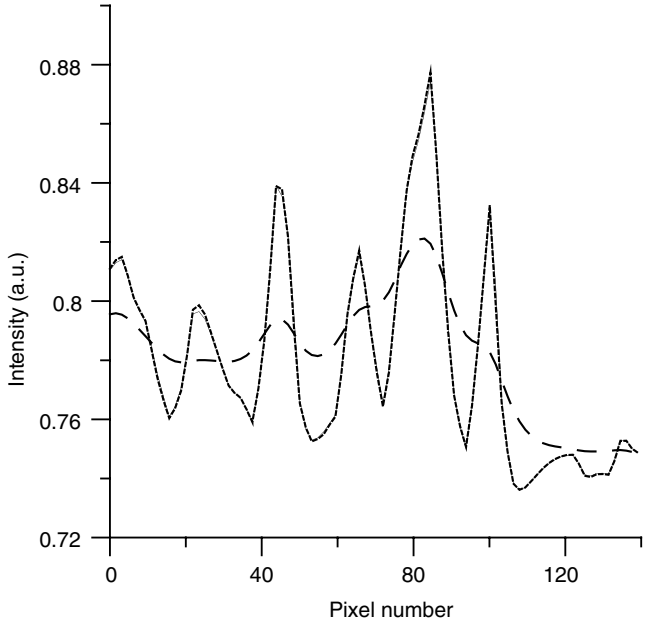

Fig. 5. Horizontal cross-sections through Fig. 4(a) (dotted line), Fig. 4(b) (dashed line), and Fig. 4(c) (solid line), taken at the same position marked with the thick white line in Fig. 4(a).

partially coherent nature of the incident illumination. Finally, in Fig. 5, we present linear cross-sections of Fig. 4(a)–(c) taken horizontally across several fur strands on Lena's hat at the same position marked in Fig. 4(a) by a thick white line. One can see that the cross-sections of Fig. 4(a) and (c) match with high precision, while the cross-section of Fig. 4(b) is substantially smoother due to the (uncompensated) effect of convolution with the PSF. This example demonstrates that a proper choice of the defocus distance in projection imaging can indeed lead to the effective cancellation of the PSF-induced blurring by the propagation-induced diffraction. An initial experiment confirming (albeit, somewhat indirectly) the presence of this effect in hard X-ray imaging with spatially incoherent polychromatic microfocus sources can be found in [15].

5. Conclusion

We have obtained new analytical expressions describing the spectral density and intensity distributions of projection images in the Fresnel region under polychromatic and spatially partially coherent Schell-model-type illumination. The results are valid for objects that can be characterised by complex transmission functions with the attenuation and phase representable as a sum of a slowly varying and a small term. Similar results have been obtained earlier in [1] in the case of monochromatic radiation. The difference between those earlier results and the present ones are also in the explicit incorporation of the magnification M (which is due to the average geometric magnification of the image in the case of a small source), incident spectral density distribution S^{in} (which depends on the degree of spectral coherence of the source and other parameters), incident phase $k\psi^{\text{in}}$ (which depends on the coherent aberrations of the illumination system), the spectral degree of coherence, g^{in}, of the incident illumination (which is a function of the spectral density distribution in the source plane and other parameters) and the detector PSF, D. We have shown that in some cases the effects of partial coherence, which usually degrade the contrast and resolution of projection images, can be utilized to counteract the Fresnel diffraction effects with the resultant images having higher spatial resolution and being free of diffraction fringes. These results can be used for optimisation with respect to contrast, resolution and signal-to-noise of projection imaging systems using polychromatic spatially partially coherent incident illumination and position-sensitive detector systems [32,33].

References

[1] T.E. Gureyev, A. Pogany, D. Paganin, S.W. Wilkins, Opt. Commun. 231 (2004) 53.
[2] J.M. Cowley, Diffraction Physics, third ed., Elsevier, Amsterdam, 1995.
[3] M. Born, E. Wolf, Principles of Optics, seventh ed., Cambridge University Press, Cambridge, 1999.
[4] M.R. Teague, J. Opt. Soc. Am. 73 (1983) 1434.
[5] A. Pogany, D. Gao, S.W. Wilkins, Rev. Sci. Instrum. 68 (1997) 2774.
[6] D. Paganin, K.A. Nugent, in: P. Hawkes (Ed.), Advances in Imaging and Electron Physics, vol. 118, Harcourt Publishers, Kent, 2001, p. 85.
[7] T.E. Gureyev, Ya.I. Nesterets, D.M. Paganin, S.W. Wilkins, J. Opt. Soc. Am. A (2006).
[8] L. Mandel, E. Wolf, Optical Coherence and Quantum Optics, Cambridge University Press, Cambridge, 1995.
[9] A. Krol, J.C. Kieffer, E. Foerster, SPIE 3157 (1997) 156.
[10] B.M. Song, S.A. Pikuz, T.A. Shelkovenko, D.A. Hammer, Appl. Opt. 44 (2005) 2349.
[11] D.R. Luke, J.V. Burke, R.G. Lyon, SIAM Rev. 44 (2002) 169.
[12] R.P. Millane, J. Opt. Soc. Am. A 7 (1990) 394.
[13] G. Gbur, E. Wolf, Opt. Lett. 27 (2002) 1890.
[14] G. Gbur, M. Anastasio, Y. Huang, D. Shi, J. Opt. Soc. Am. A 22 (2005) 230.
[15] T.E. Gureyev, A.W. Stevenson, Ya.I. Nesterets, S.W. Wilkins, Opt. Commun. 240 (2004) 81;
T.E. Gureyev, A.W. Stevenson, PCT/AU2004/001342.
[16] Y. Takayama, S. Kamada, Phys. Rev. E 59 (1999) 7128.
[17] H.H. Hopkins, Proc. Roy. Soc. Lond. A 217 (1953) 408.
[18] X. Wu, H. Liu, Med. Phys. 31 (2004) 2378.
[19] J.-P. Guigay, Opt. Commun. 26 (1978) 136.
[20] D. Paganin, S.C. Mayo, T.E. Gureyev, P.R. Miller, S.W. Wilkins, J. Microsc. 206 (2002) 33.
[21] J.P. Guigay, Optik 49 (1977) 121.
[22] L.D. Turner, B.B. Dhal, J.P. Hayes, A.P. Mancuso, K.A. Nugent, D. Paterson, R.E. Scholten, C.Q. Tran, A.G. Peele, Opt. Exp. 12 (2004) 2960.
[23] T.E. Gureyev, T.J. Davis, A. Pogany, S.C. Mayo, S.W. Wilkins, Appl. Opt. 43 (2004) 2418.
[24] D.M. Paganin, T.E. Gureyev, S.W. Wilkins, Provisional Patent No. 2004904206, Priority date July 2004.;
D.M. Paganin, T.E. Gureyev, S.W. Wilkins, in preparation.
[25] T.E. Gureyev, S. Mayo, S.W. Wilkins, D. Paganin, A.W. Stevenson, Phys. Rev. Lett. 86 (2001) 5827.
[26] S.C. Mayo, T.J. Davis, T.E. Gureyev, P.R. Miller, D. Paganin, A. Pogany, A.W. Stevenson, S.W. Wilkins, Opt. Exp. 11 (2003) 2289.
[27] T.E. Gureyev, D.M. Paganin, A.W. Stevenson, S.C. Mayo, S.W. Wilkins, Phys. Rev. Lett. 93 (6) (2004) 068103.
[28] M. Subbarao, T.C. Wei, G. Surya, IEEE Trans. Image Process. 4 (1995) 1613.
[29] M. Sanchez del Rio, R.J. Dejus, SPIE Proc. 3448 (1998) 340.
[30] J.M. Boone, T.H. Fewell, R.J. Jennings, Med. Phys. 24 (1997) 1863.
[31] S. Brennan, P.L. Cowan, Rev. Sci. Instrum. 63 (1992) 850.
[32] Ya.I. Nesterets, S.W. Wilkins, A. Pogany, A.W. Stevenson, T.E. Gureyev, Rev. Sci. Instrum. 76 (2005) 093706.
[33] S. Zabler, P. Cloetens, J.-P. Guigay, J. Baruchel, Rev. Sci. Instrum. 76 (2005) 073705.